

Cite this: *J. Mater. Chem.*, 2011, **21**, 15031

www.rsc.org/materials

PAPER

Low-temperature (below T_g) thermal bonding of COC microfluidic devices using UV photografted HEMA-modified substrates: high strength, stable hydrophilic, biocompatible surfaces

Sunanda Roy,^{ab} C. Y. Yue,^{*ab} S. S. Venkatraman^c and L. L. Ma^c

Received 21st April 2011, Accepted 28th July 2011

DOI: 10.1039/c1jm11750e

Cyclic olefin copolymer (COC) based microfluidic devices offer unique opportunities in developing high quality chips for a variety of applications but critical issues such as the bonding strength, biocompatibility and flow need to be addressed before this can be realized. In this study, we introduce a simple microfluidic device fabricated on COC (Topas) substrates that were modified by ultraviolet (UV) photo-grafting of a hydrophilic monomer 2-hydroxyethyl methacrylate (HEMA). This water soluble acrylic monomer was used to increase the bond strength, surface wettability and hemocompatibility. Thermal bonding of the microfluidic chips was accomplished at temperatures well below the glass transition temperature (T_g) of the COC polymer. Moreover, this process produced COC microchannels with modified surfaces that had stable permanent hydrophilic properties. Therefore, it can be used for Bio-MEMS applications in electrophoretic analysis where stable electro-osmotic flow (EOF) is important. The bond strength and burst pressure of the HEMA modified chips increased significantly to 1.70 MPa and 4.20 MPa for bonding at 10 °C below T_g . The COC surfaces were characterized using contact angle, EOF measurements, and Fourier transform infrared spectroscopy. The hydrophilicities of the substrates improved significantly with increase in degree of poly-HEMA immobilization and a maximum grafting yield of about 0.13% was obtained for a short irradiation time of 12 min with 25% of HEMA monomer. *In vitro* fibrinogen and fluorescent labeled bovine serum albumin adsorption results indicated that the COC surface can easily be tuned against protein adsorption by controlling the grafting yield. The *in vitro* platelet adhesion tests confirmed that the hydroxyl functionality greatly improved the surface hemocompatibility of COC by reducing the number and the degree of activation of the adherent platelets.

1. Introduction

There has been growing interest in the development of biochips based on MEMS technologies for widespread use in a wide variety of applications in diagnostics, drug sensing, and characterization of biological entities. Typically, biomaterials such as DNA, enzymes, proteins and microorganisms can be utilized in a biochip. The first generation microfluidic devices were fabricated on glass or silicon^{1,2} but due to limitations including complexity of fabrication methods, geometrical design constraints, complicated sealing process and high manufacturing cost, polymer based LAB-ON-A-CHIP devices or micro total analysis systems (μ TAS) have become hot research topics in the

field of microfluidics and BioMEMS.^{3,4} The advantages of polymers over glass and silicon as a substrate for microfluidic devices include their biocompatibility, disposability, good chemical resistance, optical properties, low cost and capacity for high-volume production⁵⁻⁷ using established manufacturing techniques such as hot embossing and injection molding.

In this regard, COC polymer based microfluidic devices offer many advantages for high quality chips due to its high glass transition temperatures (T_g s) with excellent transparency,^{8,9} low dielectric loss, low moisture absorption, and good chemical resistance. However, a few key issues need to be resolved before there can be wider adoption of COC. Firstly, a simple means to obtain high strength thermal bonds between COC substrates has to be developed to ensure that microchannels can be sealed readily. Secondly, the hydrophilic property that is rendered on the surface of COC microchannels using an appropriate treatment ought to be stable and permanent and should not vary with ageing (or storage time). This is important in order to avoid 'hydrophobic recovery'¹⁰ which has been reported in COC surfaces that were rendered hydrophilic using the plasma

^aSingapore-MIT Alliance, Manufacturing Systems and Technology Programme, Nanyang Technological University, 65 Nanyang Drive, Singapore 637460

^bSchool of Mechanical and Aerospace Engineering, Nanyang Technological University, 50 Nanyang Avenue, Singapore 639798

^cSchool of Materials Science and Engineering, Nanyang Technological University, Singapore, 639798, Singapore

modification technique. Thirdly, the modified surface that has been constructed onto the surface of COC microchannels has to be blood compatible/hemocompatible in order to evade nonspecific protein adsorption, thrombus formation or other undesirable responses. Surface modification is necessary because aqueous buffer solutions do not naturally flow readily into hydrophobic COC channels in a microfluidic device. Moreover, biological molecules absorbed by hydrophobic channel surfaces can impede flow due to clogging in the channel.

During the fabrication of a microfluidic device, the channel has to be sealed without any channel deformation and distortion. A variety of techniques such as thermal bonding,^{11–13} thermal lamination,^{14–16} ultrasonic bonding, adhesive tape,^{17,18} glue,^{19,20} and laser bonding have been employed for this purpose. The advantage of thermal bonding is that it allows the formation of homogeneous microchannels with uniform surface properties. However, the risks/susceptibilities of thermal bonding which is commonly done above T_g are that variations in the bonding temperature and pressure may destroy the dimensional integrity of the channel networks in the device without providing a strong thermal bond between the polymer substrates. For this reason, there have been attempts to develop different techniques for low temperature sealing below T_g .

Tsao *et al.*²¹ developed a low temperature bonding method for PMMA and COC using the UV/ozone treatment technique followed by thermal bonding. From their crack opening displacement tests, an increase in bond strength by about two orders in the treated samples (0.984 mJ cm^{-2} for PMMA and 0.806 mJ cm^{-2} for COC for bonding at 90°C) as compared to the untreated samples ($<0.003 \text{ mJ cm}^{-2}$ for PMMA and COC) that was attributed to high surface wetting was reported. However, the highest bond strength of COC (Zeonor 1020R, $T_g = 105^\circ\text{C}$) they obtained for thermal bonding at below T_g (at 100°C) was 0.9 mJ cm^{-2} which is lower than the bond strength for untreated Zeonor (1.1 mJ cm^{-2}) bonded at 110°C . Moreover, the drawback of this process was that the surface properties of the treated surface were unstable and its hydrophilicity changed when the treated substrates were washed using different solvents because loosely bound low molecular weight polymer products were removed. Bhattacharyya and Klapperich²² used the radio frequency plasma and ultraviolet-ozone (UVO) treatments to modify the surface of polystyrene (PS) and cyclic polyolefin copolymer (Zeonor 750R) and performed thermal bonding at below their T_g . Using the three-point bend test, they showed that UVO treatment increased the bond strength from 2 MPa and 1.5 MPa for untreated Zeonor and PS, to 8 MPa and 8.5 MPa for treated COC and PS respectively. However, their bond strength data that are based on the three-point bend test cannot be compared readily with the work done by others that are generally based either on bond strength measurements from lap shear specimens or on burst strength measurements from pressurized leak testing.

Using injection molded Topas 8007 ($T_g = 80^\circ\text{C}$) substrates, Mair *et al.*²³ conducted burst pressure measurements on chips that were thermally bonded both at T_g (80°C) and at $T_g + 15^\circ\text{C}$ (95°C). The burst pressures in the former and latter chips were 4 MPa and 12 MPa respectively (see Fig. 7 in ref. 23). However, it was apparent that there was distortion and change in shape and dimensions of their microchannels after thermal bonding

(see Fig. 8 in ref. 23). They did not study the extent of channel deformation after thermal bonding or the influence of such deformation on burst pressure. It is important to note that channel deformation during thermal bonding at above T_g should not be ignored because it can have a significant effect²⁴ on the burst pressure of the chip. In contrast, Bhagat and his co-workers²⁵ obtained a burst pressure of 1.7 MPa for their COC-5013 microfluidic device. From the above, it is apparent that much remains to be done to develop reliable techniques to obtain COC chips with high thermal bond strength. Although many COC based microfluidic devices^{26–32} have also been studied, there are limited studies on the improvement of bond strength and hemocompatibility of modified COC surfaces.

Therefore, the focus of the present work is to develop a suitable treatment that will not only lead to high thermal bond strength for bonding below T_g but will also impart durable hydrophilicity and biocompatibility to COC. The surface grafting of 2-hydroxyethyl methacrylate (HEMA) to COC utilizing the UV technique will be outlined. HEMA was selected since it has been found to reduce protein adsorption³³ and is a water soluble biocompatible monomer that can be grafted onto the surface of various polymer substrates. It will be shown that large improvements in bond strength (comparable to that for PMMA chips) and biocompatibility are obtained. Significantly, high bond strengths could be obtained for thermal bonding at temperatures well below the glass transition temperature (T_g) of the COC polymer. Although, a variety of methods such as plasma polymerization, γ -irradiation, laser treatment, ozone treatment UV-grafting have been used to functionalize^{15,34–40} the COC polymer surface, to our knowledge there has not been any study whereby HEMA has been employed as the precursor molecule in UV-photografting. Moreover, the advantage of UV-photografting is that molecular fragmentation and random chain scission that are commonly associated with other surface treatment methods can be avoided.

2. Experimental

Cyclic olefin copolymer (COC) resin, comprising Topas 5013 (Ticona, Florence, KY, US), with T_g of 130°C , was selected as the substrate material. Polymer sheets of dimensions $75 \text{ mm} \times 25 \text{ mm} \times 1 \text{ mm}$ were injection molded (Battenfeld injection molding HM 25/60) at 270°C from the pellets. Prior to injection molding, the resins were dried for 8 hours under vacuum at 20°C below their T_g to remove any moisture. The sheets were then cut into the desired sizes for further use as polymer substrates for UV-grafting. 2-Hydroxyethyl methacrylate (HEMA) of 99% purity, benzophenone (98% purity), FITC-BSA and fibrinogen from human were purchased from Sigma Aldrich, Singapore. Chemically pure grade (ACS grade) acetone, methanol and ethanol (Merck, Singapore) were used without further purification.

2.1. Preparation of COC microfluidic chips

Two types of microdevices were fabricated on the Topas 5013 substrates. The chips for the electro-osmotic flow (EOF) measurements that contained microchannels which were 6 mm long, 200 μm wide and 50 μm high (aspect ratio of 4) were

fabricated by injection molding. In contrast, the chips with the micro-mixer configuration were made by hot embossing using a Zr-based bulk metallic glass (BMG) die,⁴¹ provided by Anand's research group at MIT. Prior to embossing, the polymer substrates were annealed at 140 °C for 1 h to remove any residual stresses. Just before embossing, the substrates were cleaned using acetone and dried at ambient temperature to remove any surface contamination. The distance between any two adjacent embossed microchannels in the micro-mixer was 500 µm whereas the height and width were 40 and 50 µm respectively. Hot embossing was carried out at 140 °C and 2.94 kPa with a holding time of 4 min using a Specac hydraulic press. The patterned COC substrates were peeled off from the BMG die at room temperature, after which holes that acted as reservoirs were punched in the substrate. Finally, chips were made by thermal bonding another flat Topas 5013 substrate onto the base substrate containing the microchannels.

2.2. UV-grafting on the COC substrate

The ultra-violet (UV) grafting process was performed using a UV flood curing system (Techno Digm, Singapore). The UV ($\lambda = 365$ nm) intensity was adjusted by changing the distance from the UV lamp to the substrate. The initial weight of each substrate plate W_I was recorded. Initially, HEMA solutions with 5, 10, 15, 20, 25 and 30 wt% monomer concentration in water (or methanol) were prepared. Next, a solution containing 10 wt% of benzophenone (BP) photo-initiator in acetone was added to the above HEMA solutions and stirred to ensure good mixing. The photo-polymerization experiments were conducted using the approach by Ranby and Yang,^{42–44} where the solution mixture containing BP and monomer was deposited on the COC substrate (1 mm thick) using a micropipette. This coated substrate was then carefully covered with another piece of COC of the same size to distribute the liquid droplet uniformly. The substrates were then exposed to UV light (from the top) for a fixed duration between 1 and 20 minutes to enable the monomer to graft onto the COC surfaces. After drying at 50 °C in an oven for 45 minutes the weight of each treated substrate plate W_{II} was noted.

The substrates were then washed with hot water and methanol mixture followed by acetone to remove the residual unreacted monomer and photo-initiator and any loose homopolymer before they were dried at room temperature for 8 h. The final weight W_{III} of each sample was then measured. The grafting yield (G_Y) and grafting efficiency (GE) of HEMA on COC were determined using the following equations:^{45–47}

$$G_Y = (W_{GP}/W_I) \times 100\%, [W_{GP} = W_{III} - W_I] \quad (1)$$

$$GE = (W_{GP}/W_P) \times 100\%, [W_P = W_{II} - W_I] \quad (2)$$

where W_{GP} is the weight of the grafted polymer, W_P is the weight of the polymer formed that contains the total weight of the graft polymer and homopolymer, W_I is the initial weight of the non-grafted COC substrate, W_{II} and W_{III} are the weights of the grafted COC substrate before and after washing off.

In the context of the current work, GE is related to the efficiency of the BP and the UV process in immobilizing HEMA onto the COC surface. Some of these immobilized HEMA may

have been grafted onto the COC surface, whilst some may have joined together to form HEMA homopolymer that may not be attached to the surface. The grafting yield G_Y indicates the amount of HEMA monomer that has been grafted successfully onto the COC surface. At least 4 tests were conducted for each data point.

2.3. Surface characterizations and analysis

The chemical compositions of the unmodified and modified surfaces were determined using a Perkin-Elmer GX Fourier transform infrared spectroscope (FTIR) equipped with an attenuated total reflection (ATR) unit. The resolution was 4 cm⁻¹ and 32 scans were carried out for each run.

An X-ray photoelectron spectroscopy (Kratos Ultra XPS system) with monochromatic Al K α as an X-ray excitation source operating at 15 kV and 10 mA was used to determine the elemental compositions on the surfaces. The sampling area on the specimen was typically about 700 µm by 400 µm. A step-scan interval of 1 eV was used for wide scans, and 0.1 eV for high-resolution scans and the acquisition times were 60 s for both resolutions. The pass energies for XPS were 160 eV for wide scan and 40 eV for the detailed scan. The core-level spectra were obtained at a photoelectron takeoff angle of 90°, measured with respect to the sample surface. Binding energies were referenced to the saturated hydrocarbon peak at 285 eV.

Static water contact angle measurements were made using a video-based FTA 200 video Series contact angle apparatus. Measurements were made on a 1–2 µl droplet of de-ionized water that was placed on the surface. For each sample, at least six different spots were measured and the data were averaged.

The morphologies of both the untreated and modified COC surfaces were examined using a JEOL JSM-5600 scanning electron microscope (SEM). Prior to this, the substrates were sputtered coated for 180 s. The accelerating voltage used was 20 kV.

2.4. Thermal bonding and bond strength

Thermal bonding at between 90 °C and 130 °C was conducted using a Carver laboratory hot press. Preliminary tests were conducted to optimize the bonding pressure and bonding time in order to avoid undesirable deformation of the microchannels during thermal sealing. These parameters were then utilized to prepare specimens for the lap shear tests and burst pressure measurements. The bonding pressure and bonding time were kept constant at 3.0 MPa and 6 min respectively. Prior to bonding, the COC substrates were cleaned in ethanol and dried at room temperature. The bond strength of the modified and unmodified substrates was determined using lap shear specimens in an Instron 1130 tensile testing machine under room temperature conditions at a crosshead speed of 0.5 mm min⁻¹. The thickness of each substrate was 1 mm and the specimens had an overlap area of 15 × 10 mm². At the start of each test, the distance between the tension grips was kept constant. Eight samples were tested for each specimen condition.

2.5. Burst pressure test

The integrity of the thermal seal and the performance of the thermally sealed microdevice were assessed using a burst pressure

test. During testing, the chip was connected to a syringe pump (ISCO Teledyne Technologies Company, Model 100DM), which was fitted with a pressure transducer with an accuracy of 0.5% in the range of 0.069–68.9 MPa. To facilitate the burst test, a plastic PEEK NanoPort assembly (Science Team Services, Singapore) was glued onto the reservoirs of the thermally bonded plates using Araldite epoxy adhesive. After applying some epoxy adhesive, the substrates and the port were clamped for 24 hours at room temperature. Connections were made to the syringe pump using a natural fluoroethylene propylene (FEP) tube with a polyether ether ketone (PEEK) zero-dead-volume (ZDV) union. The ZDV union was connected to the 1/16" OD (outer diameter) tubing which can withstand a pressure rating of 41.4 MPa.

2.6. Measurement of electroosmotic flow μ_{EOF}

The current monitoring method⁴⁸ was employed to measure the electroosmotic flow (EOF) under an applied electric field of 500 V cm⁻¹. A separate set of thermally sealed microdevices containing a 60 mm long, 50 μm deep and 200 μm wide microchannel was utilized for the EOF experiments. The Tris–HCl buffer with pH 8.49 was used as the testing buffer solution. The higher ionic strength of the buffer was 20 mM phosphate, while the lower ionic strength was 19 mM phosphate. Platinum electrodes were inserted into the two reservoirs, and a voltage of 500 V was applied to the reservoir containing the 20 mM phosphate buffer. The EOF was calculated using the relationship $\mu_{\text{EOF}} = L^2/vt$, where L is the length of the channel, t is the migration time for the diluted buffer solution to reach the steady state, and v is the total applied voltage.

2.7. Surface protein adsorption

To measure the nonspecific adsorption of protein, the *in vitro* protein adsorption experiments were conducted in phosphate buffered saline (PBS) solution. Prior to adsorption, the unmodified and modified samples were hydrated in PBS for 6 h. Then the surfaces were exposed to 1 mg ml⁻¹ of FITC-BSA and 0.25 mg ml⁻¹ bovine fibrinogen respectively, for 1 h at 37 °C. The samples exposed to fibrinogen were then transferred into another 24-PS well containing fresh PBS and rinsed ~40 times by vigilant shaking. After that the samples were again transferred into other new PS wells containing 1 ml PBS and 1 wt% sodium dodecyl sulfate (SDS) in order to detach the adsorbed protein from the surface by sonication for 15 min. A Micro BCA protein assay kit (Pierce, USA) was used to quantify the eluted proteins in the SDS solution calculated from the absorbance at 562 nm using an absorptiometer (Tecan Infinite 200 series, Switzerland). On the other hand, the samples exposed to FITC-BSA (fluorescein isothiocyanate labelled bovine serum albumin) were rinsed by fresh PBS for 3–5 times and dried at room temperature for 4 h. Then surfaces were observed under fluorescent microscope. The relative fluorescent intensity of the adsorbed protein on the grafted surface was compared with the unmodified COC sample.

2.8. Platelet adhesion

The interactions between blood and the COC samples were studied using the platelet adhesion experiment. The experiments

were conducted using fresh platelet-enriched plasma (PRP) that was isolated from human blood by centrifugation at 1000 rpm for 10 min. The platelets were suspended in a buffer solution that had a concentration of 7×10^9 platelets per ml. Both the unmodified and modified samples (each with a surface area of 10 mm \times 10 mm) were placed into a 24-PS well. Then, 30 μl of fresh platelet-rich plasma (PRP) was carefully dropped onto the top of each sample surface. After incubation for 60 min at 37 °C, the surfaces were carefully and slowly rinsed several times using PBS (pH 7.4). After thorough washing, the platelets that adhered to the untreated and grafted surfaces were fixed with 2.5% glutaraldehyde/PBS solution for 1 hour, followed by the dehydration procedure using a series of different concentrations of ethanol–water mixtures (0, 30, 40, 50, 60, 70, 80, 90, 100 vol% of ethanol) for 30 min. These surfaces were then examined at a magnification of 1500 \times in a JEOL JSM-5600 scanning electron microscope (SEM), and the number of platelets per unit surface area was determined.

3. Results and discussion

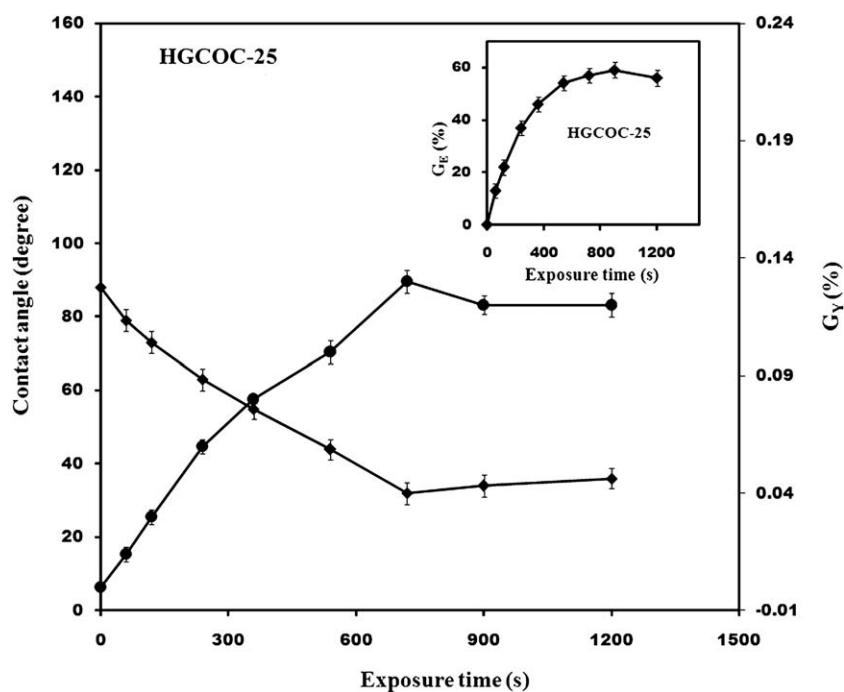
3.1. Grafting yield and efficiency

The influence of HEMA concentration on the grafting efficiency (GE) and the grafting yield (G_Y) for 10 wt% BP at a constant UV exposure time of 720 seconds is summarized in Table 1. The BP concentration of 10 wt% was selected because preliminary tests had indicated that higher levels of BP lowered the grafting yield due to the uncontrolled acceleration of homopolymer formation and termination reaction by the initiated monomer radicals. It can be seen in Table 1 that G_Y increases with increase in HEMA concentration and reached a peak value of 0.13% at 25 wt% HEMA. The drop in G_Y at higher concentrations of HEMA indicated that higher monomer concentration enhanced the rate of homopolymer formation rather than surface graft polymerization. Based on this, most of our studies will focus on COC surfaces that were modified by UV grafting using 25 wt% and 10 wt% BP (denoted as HGCOC-25 treatment condition).

The effect of UV exposure time on G_Y and the contact angle for the HGCOC-25 condition is shown in Fig. 1. It can be seen that G_Y increased with increasing irradiation time reaching a peak value of 0.13% at 720 seconds after which it plateaued off to a value of 0.11%. The slightly lower values of grafting yield G_Y with longer irradiation time has been attributed to photo-degradation of the grafted polymer chains due to prolonged exposure to UV light.⁴⁴ Moreover, it is apparent from the inset in Fig. 1 that the grafting efficiency (GE) increased with irradiation time reaching a peak value of 60% at 900 seconds before decreasing slightly at longer times. The continued increase in GE beyond 720 seconds, at which G_Y attained a maximum value, indicated that there was some cross-linking between the monomers, and between the monomers and grafted polymers. It can be seen from Fig. 1 that the contact angle dropped from 88° for untreated COC to between 32° and 35° ($\pm 3^\circ$) for the modified surface after an irradiation time of 720 seconds. This clearly indicated that UV-photografting of the COC surface using HEMA increased the surface hydrophilicity. It is also evident from Table 1 that the lowest contact angle was obtained with 25 wt% HEMA treatment.

Table 1 Effect of monomer concentrations on the grafting yield, grafting efficiency and hydrophilicity for the photografting of HEMA onto COC surface

Sample type	HEMA (%)	BP (%)	Time/s	G_Y (%)	GE (%)	Contact angle/ $^\circ$
Untreated	0	0	0	0	0	88 ($\pm 2.5^\circ$)
HGCOC-5	5	10	720	0.03 (± 0.005)	19 (± 3.1)	76 ($\pm 2.6^\circ$)
HGCOC-10	10	10	720	0.07 (± 0.005)	41 (± 3.4)	53 ($\pm 2.6^\circ$)
HGCOC-15	15	10	720	0.10 (± 0.005)	50 (± 3.8)	39 ($\pm 2.6^\circ$)
HGCOC-20	20	10	720	0.11 (± 0.006)	54 (± 4.0)	36 ($\pm 2.8^\circ$)
HGCOC-25	25	10	720	0.13 (± 0.006)	57 (± 3.9)	32 ($\pm 3.0^\circ$)
HGCOC-30	30	10	720	0.11 (± 0.007)	60 (± 4.2)	35 ($\pm 3.0^\circ$)

**Fig. 1** Effects of UV irradiation time on the contact angle and grafting yield for HGCOC-25 sample (the inset diagram shows the change of grafting efficiency with identical exposure time from 60 to 1200 seconds).

3.2. Bond strength test and burst test

It is apparent from Fig. 2 that all the UV photografted samples could be thermally bonded at between 90 °C and 130 °C at temperatures significantly below the T_g (130 °C) of the Topas substrate. It can be seen from Fig. 2a that the grafted samples had very good bond strength and the lowest possible bonding temperature was 90 °C. The bond strength for the grafted substrates at 90 °C was 0.51 MPa which was comparable to that (0.64 MPa) for the untreated COC that was thermally bonded at 120 °C. The bond strength increased with increasing bonding temperature (see Fig. 2a) reaching a considerably high value of 2.10 MPa at 130 °C which corresponds to the T_g . The above compared very favorably with thermal bonding in the untreated COC samples which could only be accomplished at temperatures of 120 °C and higher.

It is interesting to note that grafted samples that were bonded at 95 °C possess ~10% higher bond strength than the non-grafted samples that were bonded at 120 °C. Moreover, the bond strength of grafted samples that were bonded at 120 °C and 130 °C exhibited bond strengths that were 165% and 150% higher compared to their corresponding unmodified

counterparts. Clearly, surface modification of COC by UV grafting using HEMA monomer permits high bond strengths to be obtained for bonding at temperatures well below T_g without causing any deformation of the microchannels in microfluidic devices.

The burst pressure test data for COC chips prepared from the different grafted samples are shown in Fig. 2b. It is apparent from Fig. 2b that the burst pressure strength increased significantly with increasing bonding temperature. The chip that was bonded at 120 °C exhibited a very high burst pressure of 4.20 MPa. The thermal bond in the HEMA modified chips that were bonded at 130 °C was so high that all the samples for this bonding temperature failed at the connector joints of the testing equipment (at pressures above 5 MPa). The burst pressure for the HEMA modified chip that was bonded at 110 °C (~3.65 MPa) and 120 °C (~4.23 MPa) was 2.1 and 2.5 times higher respectively, as compared to the untreated chip (1.71 MPa) that was bonded at 120 °C. It is evident that UV grafting with HEMA is a very effective way of producing strong and robust COC microfluidic devices.

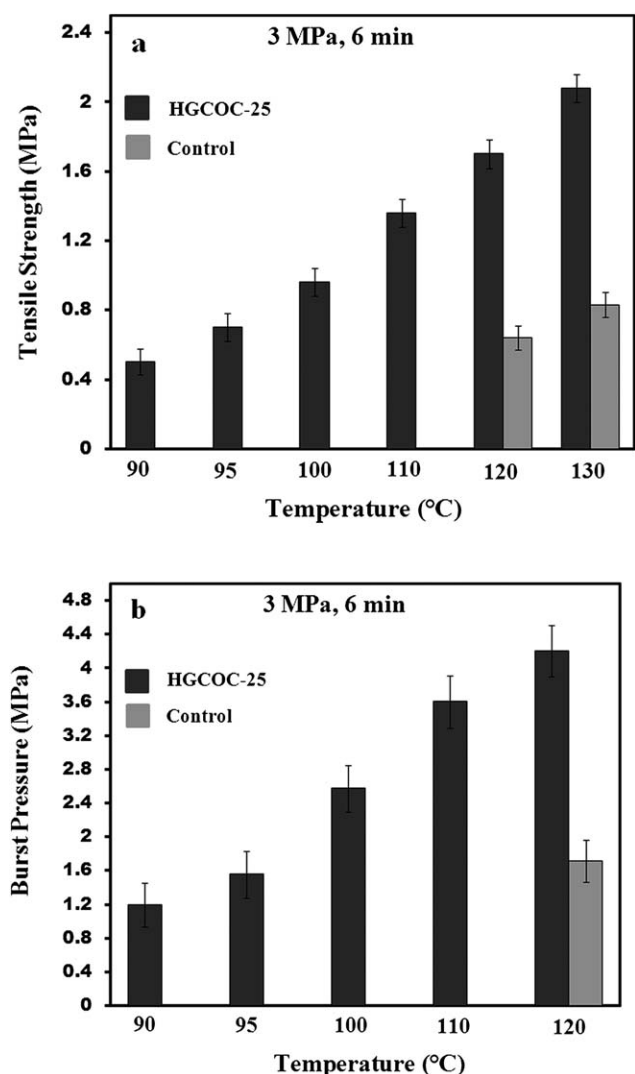


Fig. 2 The effect of bonding temperature on the (a) lap shear strength and (b) burst pressure strength for HGCOC-25 specimen.

3.3. Surface characterization and analysis

The influence of the HEMA monomer concentration on the degree of surface grafting on the COC surface will now be examined using the surface analysis results. The FTIR-ATR spectra of the pure monomer, untreated COC and HEMA grafted COC (HGCOC) are shown in Fig. 3. The absorption peaks at 1724 cm^{-1} and 3422 cm^{-1} for the HGCOC samples in Fig. 3 indicated the presence of the HEMA ester and hydroxyl (O–H) groups respectively. The peak at 1636 cm^{-1} in the monomer (see Fig. 3(ii)) corresponds to the unsaturated C–C double bond. It is interesting to note that this peak disappeared after UV grafting which indicated that the C–C double bond was utilized for the HEMA surface modification. Moreover, the carbonyl peak position was shifted from 1714 cm^{-1} in pure monomer to 1724 cm^{-1} in the HEMA modified COC which also indicated the absence of α – β unsaturation in the grafted surfaces. The high intensities for the OH and C=O peaks in the pure monomer solution were consistent with the presence of these bonds in HEMA. The gradual increase of the hydroxyl (OH) and

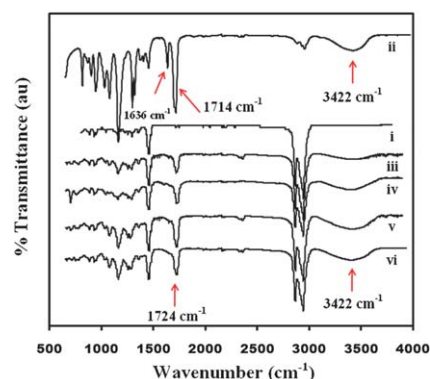


Fig. 3 Typical ATR-FTIR spectra of untreated COC, HEMA monomer and UV-grafted COC surfaces: (i) control, (ii) HEMA monomer, (iii) HGCOC-10, (iv) HGCOC-15, (v) HGCOC-25 and (vi) HGCOC-30.

keto (C=O) peaks in the grafted COC in Fig. 3(iii)–(v) indicated that the extent of HEMA grafting on the modified surface increased when the monomer concentration was increased from 5 wt% to 25 wt%.

Fig. 4 demonstrates the survey spectrum of virgin COC and COC that had been modified with solutions with several different HEMA concentrations. The XPS spectrum of the virgin COC had a small oxygen peak at a binding energy (BE) of 536 eV which represents the intrinsic low-level oxidized carbon state on the COC surface. The common peak at 285.1 eV that was present in all the COC samples can be assigned to the binding energy of C1s. Fig. 4 clearly shows that after surface modification, the height of the oxygen peak increased drastically. Detailed elemental analysis showed that the HGCOC-25 surface composed of 27% and 73% of atomic oxygen and carbon respectively (data not shown), whereas the untreated COC surface contained 6% oxygen and 94% carbon. Therefore, it is apparent that the amount of oxygen on the grafted COC surfaces increased as the grafting yield of HEMA increased with increasing monomer concentrations.

Fig. 5a shows the high resolution C1s XPS spectra of HGCOC-25 surface. The broad C1s peak has been resolved into three components representing C atoms attached to other C and O atoms. The binding energy values 285 eV, 286.5 eV and 289.1 eV corresponding to C–H or C–C, C–OH and O–C=O, respectively. Similarly, Fig. 5b shows the O 1s spectra of HGCOC-25 that is fitted with three subpeaks at 531.8 eV (C=O), 532.5 eV (O–H) and 533.4 eV (CO–O–C). However, the XPS spectra (C1s) for untreated COC exhibited two peaks only as previously demonstrated.^{10,49}

3.4. Microchannel dimensional integrity after thermal bonding

To confirm that the microchannels were thermally sealed without any distortion in channel geometry and no change in channel dimensions, polished cross-sections of the chips were examined under the SEM. It can be seen from Fig. 6a that both the dimensional and geometrical integrity of the channel were maintained after thermal bonding for 6 min at 110 °C under 3 MPa bond pressure. It is apparent from the inset in Fig. 6a which shows a magnified picture of the interface that the side walls of

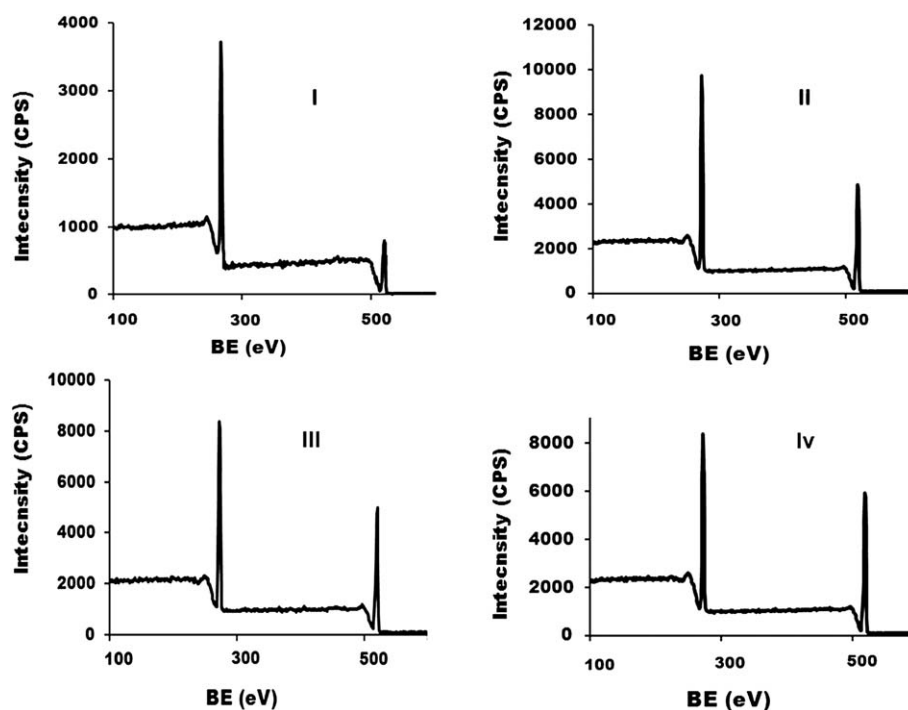


Fig. 4 Typical XPS spectra of the untreated and UV grafted COC surfaces: (i) control, (ii) HGCO-10, (iii) HGCO-15, and (iv) HGCO-25.

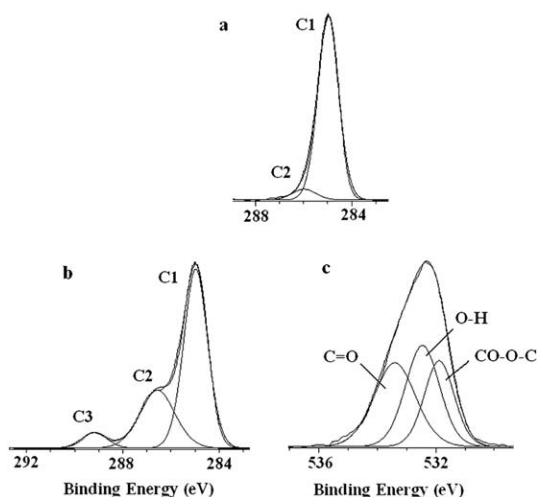


Fig. 5 Core-level XPS spectra for (a) C1s control, (b) C1s HGCO-25 and (c) O 1s HGCO-25.

the bonded microchannel remained straight. Fig. 6b shows a micrograph of a microchannel that has been injected with a fluorescent protein solution of FITC-BSA that was prepared using PBS (pH 7.4). The purpose of using the fluorescent proteins was twofold: to determine the protein adsorption, and to facilitate assessment of any leakage during the pressure test. It was apparent from Fig. 6 that good sealing was obtained without causing any leak or shape distortion of the microchannel during the encapsulation process by thermal bonding. This serves to further confirm that surface grafting of COC using HEMA is an effective way to establish low temperature thermal sealing of microfluidic devices.

3.5. Protein adsorption

Fig. 7a shows the amount of fibrinogen adsorption on the surface of modified COC prepared under different HEMA monomer concentrations. It is apparent from Fig. 7a that the adsorbed amount of fibrinogen decreased from $0.69 (\pm 0.08) \mu\text{g cm}^{-2}$ to $0.45 (\pm 0.08) \mu\text{g cm}^{-2}$ with increase in HEMA monomer concentrations. Fig. 7b shows the fluorescent intensity of the FITC-BSA adsorbed on the modified COC surfaces. The intensity of fluorescent light indicates the amount of protein adsorption. The lower intensity of fluorescent light with increasing HEMA monomer concentration indicated that the surfaces that had been modified using more HEMA are less sensitive to protein adsorption. On the other hand, the high fluorescent intensity from unmodified COC surface indicated substantial protein adsorption on that surface. The suppression of protein adsorption with monomer concentration can be attributed to the increase in grafting yield.⁵⁰ Thus, such significant reduction in protein revealed that COC surface grafted with HEMA would be an important technique in the field of capillary electrophoretic separation of proteins and peptides. A detail study on capillary electrophoresis based on HGCO-25 will be reported separately.

3.6. Blood platelets adhesion

Platelet adhesion is of the most important phenomena in determination of the biocompatibility of the materials. In this study, *in vitro* platelet adhesion experiments were used to evaluate the blood compatibility of the grafted COC substrates. The assessment of platelet adhesion is important because the tendency for platelet adhesion affects the thrombogenicity of blood when it is in contact with a biomaterial surface. Thrombus formation on blood contacting surfaces is undesirable as it can cause

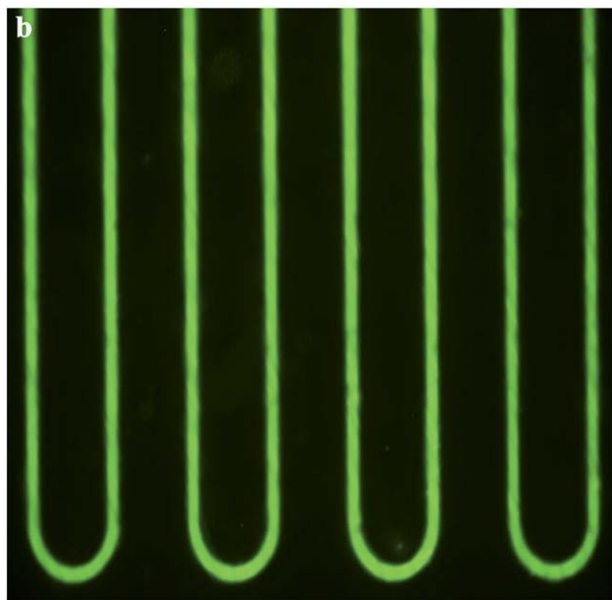
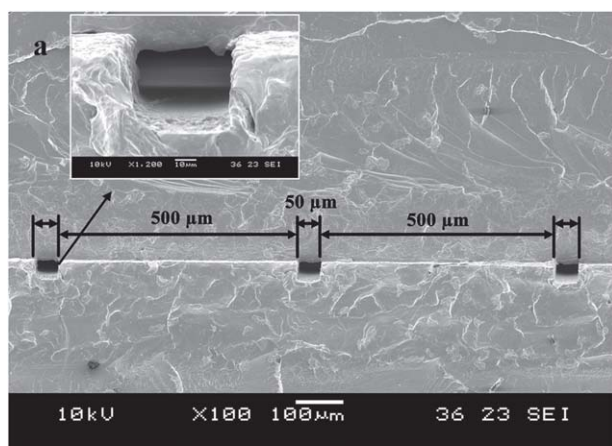


Fig. 6 (a) SEM micrograph of cross-section of a thermally sealed microdevice showing good integrity of the microchannels (bonding temperature = 110 °C, bonding pressure = 3 MPa, bonding time = 6 min); (b) microchannels in micromixer that were filled with FITC-BSA solution indicating good sealing with no leakage.

restriction of blood flow.⁵¹ Therefore, a surface that exhibits little or no platelet adhesion is highly desirable for microfluidic devices. Typical SEM micrographs of adherent platelets on the untreated and HEMA grafted COC surfaces are shown in Fig. 8. It is apparent that the unmodified COC surface had many more adhered platelets, and that some of the platelets formed aggregates (see Fig. 8a) that are commonly called thrombi. Moreover, some deformed platelets which consisted of platelets with some radiating white streaks (commonly called pseudopodia) were present on the untreated COC surface. In contrast, there was significantly less platelet distortion and adhesion on the surfaces of grafted substrates. It can be seen for the HGCOC-25 substrate (see Fig. 8b) that the few adhered platelets that existed were mostly isolated and round, which indicated that the HEMA polymer graft reduced the degree of activation of the COC surface to platelet adhesion. However, the sample in Fig. 8c

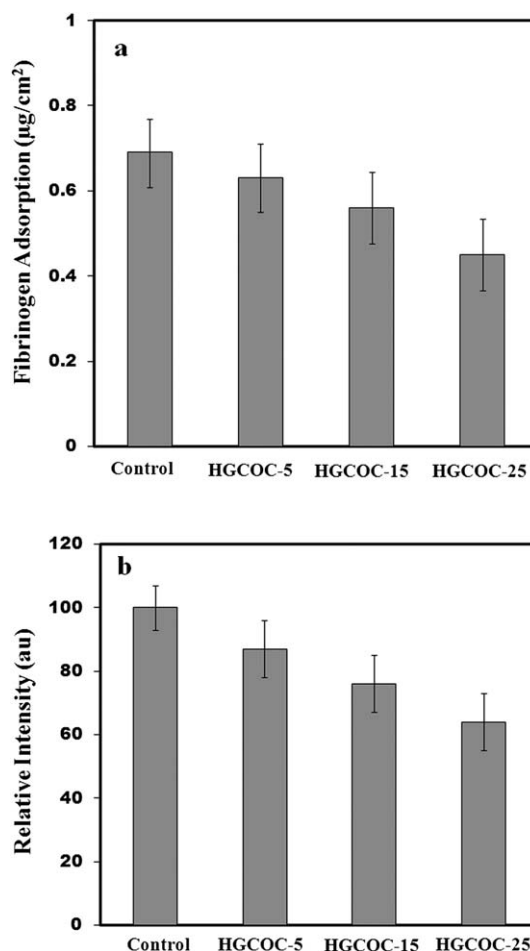


Fig. 7 Influence of monomer concentration in the HEMA grafted COC on (a) the amount of *in vitro* fibrinogen and (b) FITC-BSA adsorbed.

which was also grafted with 25 wt% HEMA solution but irradiated to UV for 1200 seconds showed a slightly higher number of adhered platelets with some small thrombi. This may be due to the higher surface roughness (43 nm) in the latter sample.

The statistical results for platelet adhesion on the different surfaces are given in Table 2. It can be seen from Table 2 that the amount of adhered platelets per unit surface area of the COC sample decreased sharply with increase in HEMA monomer concentration. This is probably related to both the hydrophilicity and difference in HEMA content of the modified COC surfaces. It was noted that the platelet adhesion for the HGCOC-25 and HGCOC-30 samples was similar which indicated that the optimal surface properties have been attained. Hence, it is evident that the hemocompatibility of COC can be improved by using HEMA surface grafting.

3.7. Electroosmotic mobility (μ_{eo})

Table 3 shows the results of EOF mobility in the untreated chip, freshly prepared HEMA-grafted chip and aged HEMA-grafted chips. The grafted HEMA polymer affects the surface charge density and ζ potential of the modified surface and hence will have an influence of the EOF in the microchannel. It can be seen

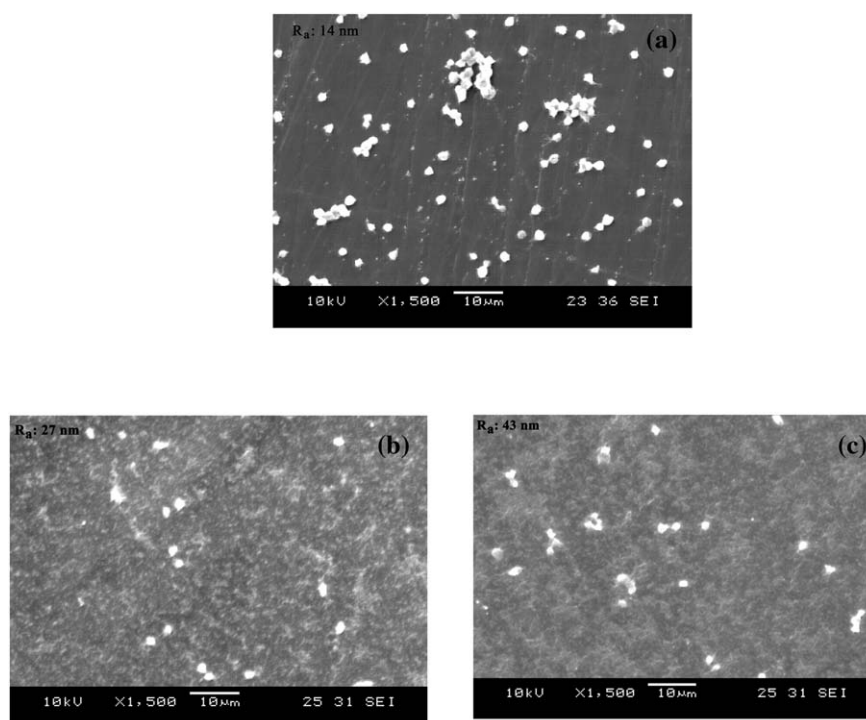


Fig. 8 Typical SEM micrographs of untreated and UV treated COC surfaces after platelet adhesion for 60 min: (a) control surface, (b) UV grafted surface with 25% HEMA for 720 seconds, and (c) UV grafted surface with 25% HEMA for 1200 seconds.

Table 2 Number of adhered platelets on various UV grafted COC surfaces

Sample	No. of adhered platelets/mm ²
Untreated	>136 (± 10)
HGCOC-5	121 (± 10)
HGCOC-10	103 (± 10)
HGCOC-15	90 (± 8)
HGCOC-20	69 (± 8)
HGCOC-25	50 (± 4)
HGCOC-30	46 (± 4)

in Table 3 that the EOF in the untreated microchannels was $3.60 \times 10^{-4} \text{ cm}^2 \text{ V}^{-1} \text{ s}^{-1}$ and was significantly increased to $7.71 \times 10^{-4} \text{ cm}^2 \text{ V}^{-1} \text{ s}^{-1}$ for the HEMA grafted HGCOC-25 sample. No significant difference in EOF mobility was observed between the freshly UV grafted samples and aged samples that had been stored at room temperature for 21 days. This indicated that the surface properties of the HEMA grafted COC chips are highly stable and will not be affected by ageing due to storage.

4. Conclusions

A suitable treatment that not only leads to high bond strength for thermal bonding below T_g but that will also impart durable hydrophilicity and biocompatibility to COC has been developed. This was achieved by surface grafting 2-hydroxyethyl methacrylate (HEMA) monomer to COC utilizing the UV photo-technique. Significant improvements in bond strength and biocompatibility were obtained with HEMA grafting by using a solution containing 10 wt% benzophenone (BP) initiator and 25 wt% HEMA and an UV irradiation time of 720 seconds. Critically, using this method we were able to produce a stable hydrophilic surface and improve the reproducibility of analysis and stability of EOF for the microchip electrophoresis. Hence, HEMA coated COC microchips can be utilized widely in BioMEMS applications in the analysis of biomolecules.

Acknowledgements

Research funding through the Singapore-MIT Alliance (SMA) Flagship Research Project in the Manufacturing Systems and Technology Program is acknowledged. S. Roy is grateful for

Table 3 Electroosmotic mobility for UV grafted COC microchannels (40 μm deep and 60 mm long) modified with different monomer concentrations

Channel condition (HEMA grafted)	No. of measurements	EOF/ $10^{-4} \text{ cm}^2 \text{ V}^{-1} \text{ s}^{-1}$		
		Fresh sample	Sample after 21 days aging	Contact angle after 21 days aging ($\pm 3^\circ$)
Untreated	7	3.60 ± 0.38	3.60 ± 0.38	88
HGCOC-25	5	7.71 ± 0.41	7.43 ± 0.38	35

financial support through an SMA Graduate Fellowship. We also acknowledge L. Anand for providing the BMG micromixer mold.

References

- 1 S. C. Terry, J. H. Jerman and J. B. Angell, *IEEE Trans. Electron Devices*, 1979, **ED-26**, 1880–1886.
- 2 A. T. Wooly and R. A. Mathies, *Anal. Chem.*, 1995, **67**, 3676–3680.
- 3 R. M. McCormick, R. J. Nelson, M. G. Alonso-Amigo, D. J. Benvegnu and H. H. Hooper, *Anal. Chem.*, 1997, **69**, 2626–2630.
- 4 D. J. Harrison, Z. Fan, K. Seiler and K. Flurri, *Proc. Transducers 93*, Yokohama, Japan, 1993, p. 403.
- 5 J. McDonald, D. Duffy, J. Anderson, D. Chiu, H. Wu, O. Schueller and G. Whitesides, *Electrophoresis*, 2000, **21**, 27–40.
- 6 H. Becker and C. Gartner, *Anal. Bioanal. Chem.*, 2008, **390**, 89–111.
- 7 H. Becker and C. Gartner, *Electrophoresis*, 2000, **21**, 12–26.
- 8 T. Rohr, D. F. Ogletree, F. Svec and J. M. J. Frechet, *Adv. Funct. Mater.*, 2003, **13**, 264–270.
- 9 G. Khanarian, *Opt. Eng. (Boca Raton, FL, U. S.)*, 2001, **40**, 1024–1029.
- 10 S. Roy, C. Y. Yue, Y. C. Lam, Z. Y. Wang and H. Hu, *Sens. Actuators, B*, 2010, **150**, 537–549.
- 11 B. Y. Peng, C. W. Wu, Y. K. Shen and Y. Lin, *Polym. Adv. Technol.*, 2010, **21**, 457–466.
- 12 A. Muck, J. Wang, M. Jacobs, G. Chen, M. P. Chatrathi, V. Jurka, Z. Vyborny, S. D. Spillman, G. Sridharan and M. J. Schoning, *Anal. Chem.*, 2004, **76**, 2290–2297.
- 13 J. Y. Cheng, C. W. Wei, K. H. Hsu and T. H. Young, *Sens. Actuators, B*, 2004, **99**, 186–196.
- 14 H. Klank, J. P. Kutter and O. Geschke, *Lab Chip*, 2002, **2**, 242–246.
- 15 M. A. Roberts, J. S. Rossier, P. Bercier and H. Girault, *Anal. Chem.*, 1997, **69**, 2035–2042.
- 16 Z. Wu, N. Xanthopoulos, F. Reymond, J. S. Rossier and H. H. Girault, *Electrophoresis*, 2002, **23**, 782–790.
- 17 P. Martin and D. Matson, *Proc. SPIE Microfluidic Devices*, 1998, vol. 3515, pp. 172–176.
- 18 S. Satyanarayana, R. N. Karnik and A. Majumdar, *J. Microelectromech. Syst.*, 2005, **14**, 392–399.
- 19 D. S. Soane, Z. M. Soane, H. H. Hooper, M. G. Alonso-Amigo, *US Pat. no. 6 176 962*, 2001.
- 20 S. Schlautmann, G. A. J. Besselink, P. G. Radhakrishna and R. B. M. Schasfoort, *J. Micromech. Microeng.*, 2003, **13**, 81–84.
- 21 C. W. Tsao, L. Hromada, J. Liu, P. Kumar and D. L. DeVoe, *Lab Chip*, 2007, **7**, 499–505.
- 22 A. Bhattacharyya and C. M. Klapperich, *Lab Chip*, 2007, **7**, 876–882.
- 23 D. A. Mair, E. Geiger, A. P. Pisano, J. M. J. Frechet and F. Svec, *Lab Chip*, 2006, **6**, 1346–1354.
- 24 Z. Y. Wang, C. Y. Yue, Y. C. Lam, S. Roy and R. K. Jena, A modified quasi-creep model for assessment of deformation of Topas COC substrates in the thermal bonding of microfluidic devices, *J. Appl. Polym. Sci.*, 2011, **122**, 867–873.
- 25 A. A. S. Bhagat, P. Jothimuthu, A. Pais and I. Papautsky, *J. Micromech. Microeng.*, 2007, **17**, 42–49.
- 26 J. Steigert, S. Haeberle, T. Brenner, C. Mueller, C. P. Steinert, P. Koltay, N. Gottschlich, H. Reinecke, J. Ruehe, R. Zengerle and J. Ducee, *J. Micromech. Microeng.*, 2007, **17**, 333–341.
- 27 K. Zhou and I. Papautsky, *Proc. SPIE-Int. Soc. Opt. Eng.*, 2007, **6465**, 64650R.
- 28 T. Nielsen, D. Nilsson, F. Bundgaard, P. Shi, P. Szabo, O. Geschke and A. Kristensen, *J. Vac. Sci. Technol., B*, 2004, **22**, 1770–1775.
- 29 B. Bilenberg, M. Hansen, D. Johansen, V. Özkapici, C. Jeppesen, P. Szabo, I. M. Obieta, O. Arroyo, J. O. Tegenfeldt and A. Kristensen, *J. Vac. Sci. Technol., B*, 2005, **23**, 2944–2949.
- 30 G. A. Diaz-Quijada, R. Peytavi, A. Nantel, E. Roy, M. G. Bergeron, M. M. Dumoulin and T. Veres, *Lab Chip*, 2007, **7**, 856–862.
- 31 T. L. Wallow, A. M. Morales, B. A. Simmons, M. C. Hunter, K. L. Krafcik, L. A. Domeier, S. M. Sickafoose, K. D. Patel and A. Gardea, *Lab Chip*, 2007, **7**, 1825–1831.
- 32 K. S. Ma, F. Reza, I. Saaem and J. Tian, *J. Mater. Chem.*, 2009, **19**, 7914–7920.
- 33 M. Tanaka, T. Motomura, M. Kawada, T. Anzai, Y. Kasori, T. Shiroya, K. Shimura, M. Onishi and A. Mochizuki, *Biomaterials*, 2000, **21**, 1471–1481.
- 34 D. Nikolova, E. Dayss, G. Leps and A. Wutzler, *Surf. Interface Anal.*, 2004, **36**, 689–693.
- 35 S. J. Hwang, M. C. Tseng, J. R. Shu and H. H. Yu, *Surf. Coat. Technol.*, 2008, **202**, 3669–3674.
- 36 B. L. Johansson, A. Larsson, A. Ocklind and A. Ohrlund, *J. Appl. Polym. Sci.*, 2002, **86**, 2618–2625.
- 37 W. J. Huang, F. C. Chang and P. P. J. Chu, *Polymer*, 2000, **41**, 6095–6101.
- 38 Q. Pu, O. Oyesanya, B. Thompson, S. Liu and J. C. Alvarez, *Langmuir*, 2007, **23**, 1577–1583.
- 39 T. B. Stachowiak, D. A. Mair, T. G. Holden, L. J. Lee, F. Svec and J. M. Fréchet, *J. Sep. Sci.*, 2007, **30**, 1088–1093.
- 40 C. Li, Y. Yang, H. G. Craighead and K. H. Lee, *Electrophoresis*, 2005, **26**, 1800–1806.
- 41 D. L. Henann, V. Srivastava, H. K. Taylor, M. R. Hale, D. E. Hardt and L. Anand, *J. Micromech. Microeng.*, 2009, **19**, 115030.
- 42 W. Yang and B. Ranby, *J. Appl. Polym. Sci.*, 1996, **62**, 545–555.
- 43 W. T. Yang and B. Ranby, *Polym. Bull.*, 1996, **37**, 89–96.
- 44 W. Yang and B. Ranby, *J. Appl. Polym. Sci.*, 1996, **62**, 533–543.
- 45 P. Yang, J. Deng and W. Yang, *Macromol. Chem. Phys.*, 2004, **205**, 1096–1102.
- 46 J. Jang and W. S. Go, *Fibers Polym.*, 2008, **9**, 375–379.
- 47 M. A. Khan, S. K. Bhattacharia, M. H. Kabir, A. M. S. A. Chowdhury and M. M. Rahman, *Polym.-Plast. Technol. Eng.*, 2005, **44**, 1079–1093.
- 48 X. Huang, M. Gordon and R. N. Zare, *Anal. Chem.*, 1988, **60**, 1837–1838.
- 49 S. Roy and C. Y. Yue, *Plasma Processes Polym.*, 2011, **8**, 432–443.
- 50 R. Iwata, P. Suk-In, V. P. Hoven, A. Takahara, K. Akiyoshi and Y. Iwasaki, *Biomacromolecules*, 2004, **5**, 2308–2314.
- 51 S. L. Llopis, J. Osiri and S. A. Soper, *Electrophoresis*, 2007, **28**, 984–993.